# Surface Modification of Halogenated Polymers. 7. Local Reduction of Poly(tetrafluoroethylene) and Poly(chlorotrifluoroethylene) by a Scanning Electrochemical Microscope in the Feedback Mode

**Catherine Combellas,* Jalal Ghilane, Frédéric Kanoufi, and Driss Mazouzi**

*Laboratoire Environnement et Chimie Analytique, UMR 7121, 10 rue Vauquelin, 75231 Paris Cedex 05, France*

*Received: December 3, 2003; In Final Form: March 1, 2004*

Fluoropolymers have been reduced locally by the radical anion of a redox mediator electrogenerated at a microelectrode operating in the configuration of a scanning electrochemical microscope. Approach curves with different redox mediators were used to investigate the reduction mechanism of the fluoropolymer. Different factors are discussed, such as the monomer reduction mechanism, the kinetic control by the surface modification growth, and the conductivity of the modified surface. The fluoropolymers' reduction parallels the trends observed in organic electrochemistry in solution within the haloalkane series.

## 1. Introduction

The chemical reduction processes of fluoropolymers were discovered in the 1950s, but the mechanism is not completely clear yet.[1,2] However, whatever the reductive treatment, most authors agree that it results in the carbonization of the polymeric material,[1−20] and the formation of poly(fluoroacetylene) has also been mentioned.[21]

When reduction is achieved in the vicinity of an electrode in the presence of a supporting electrolyte, carbonization may be represented by

$$-(CF_2-)_n + (2n)e^- + (2n)Cat^+ \rightarrow -(C-)_n + (2n)[Cat^+,F^-] \quad (1)$$

in the case of poly(tetrafluoroethylene) (PTFE), with $Cat^+$ the cation of the electrolyte.

It is followed by charging of the polymeric carbon:

$$-(C-)_n + (\delta n)e^- + (\delta n)Cat^+ \rightarrow [-(C^{\delta-}-)_n,(\delta n)Cat^+] \quad (2)$$

The reaction leads to an *n*-doped polymeric carbon-based material with both electronic[22−24] and ionic[25] conductivities.[1,2] The latter conducting material is responsible for the propagation of charges and therefore the reductive carbonization process inside the material.

The indirect reduction of PTFE by an electrogenerated radical anion ($P^{\bullet-}$)

$$P + e^- \rightarrow P^{\bullet-} \text{ (standard reduction potential } E_P{}^0) \quad (3)$$

may be studied by a microelectrode held in the close vicinity of the polymer surface.

This situation was investigated via an ultramicroelectrode band mounted in the same plane as the polymeric surface.[26] This mounting device operating in a double-band assembly fashion allowed thorough comprehension of the polymer reduction by strong reducing agents. Again under such circumstances the conductivity of the carbonized material allowed the reduction propagation into the bulk material. It has been shown that the reductive process was then kinetically controlled by the conductivity of the *n*-doped material (eq 2). The reduction of the surface led to its local carbonization according to the following global equation:

$$-(CF_2-)_n + [(2+\delta)n]P^{\bullet-} + [(2+\delta)n]Cat^+ \rightarrow [-(C^{\delta-}-)_n,(\delta n)Cat^+] + (2n)[Cat^+,F^-] + [(2+\delta)n]P \quad (4)$$

where the radical anion acts as a relay for the indirect charging of the carbonized material.

However, under such conditions, it was not possible to work under kinetic control by the reduction of PTFE (eq 1) since it would have led to reduced current efficiencies, which are difficult to study experimentally.

A scanning electrochemical microscope (SECM) in the feedback mode is known to be a more appropriate tool to investigate heterogeneous reaction kinetics.[27−30] Indeed, in a typical experiment, a microelectrode disk is held in regard to the substrate surface and moved toward it while a stable redox active species such as a reducing agent is generated. The microelectrode feedback current depends on the rate of the electron transfer at the solution−substrate interface. Owing to its experimental configuration, the SECM provides a current efficiency of 1,[31] and then allows the measurement of a wider range of kinetics than the double-band systems. Indeed, higher and lower feedback currents can be detected by the SECM, which correspond to faster and slower kinetics, respectively.

Here, we have used a homemade SECM to induce local reduction of fluoropolymers. A reducer, $P^{\bullet-}$, the stable radical anion of a redox mediator, P, was electrogenerated at a microcathode that approached the fluoropolymer surface. The principle of the fluoropolymer reduction in the SECM configuration is presented in Figure 1, where (i) the charge transfer at the liquid−polymer interface and (ii) the growth of the reduced polymer phase are schematized. Step ii proceeds efficiently owing to easy charge transport into the black carbonized phase and charge transfer at the carbonaceous material−fluoropolymer interface. Different redox mediators were used (Table 1) to assess the potential dependency of the charge transfer to the

10.1021/jp0376929 CCC: $27.50 
Published on Web 04/24/2004

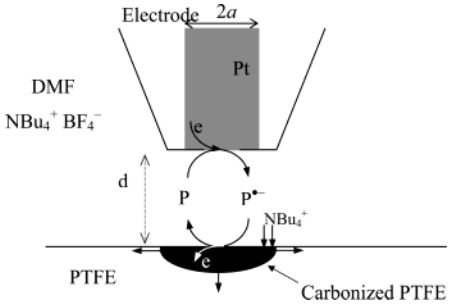


**Figure 1.** Schematic illustration of the localized reduction of a fluoropolymer surface (here PTFE) by an SECM and of growth of the carbonized area.

fluoropolymer. It should provide some interesting information for the extension of the electron-transfer theory to the interface between a solution and a solid polymer phase.

In this paper, we have focused on the investigation of the mechanism of charge transfer to fluoropolymers by using the approach curves obtained in the feedback mode of the SECM. The polymers investigated were PTFE and poly(chlorotrifluorethylene) (PCTFE; monomer $CF_2CFCl$). From the latter, we expected to observe the effect of the C−X (X = F or Cl, respectively) bond strength on the polymer reducibility. The SECM characterization of the *n*-doped material formed upon the polymer reduction is also discussed.

## 2. Experimental Section

The PTFE and PCTFE samples were plaques (diameter 2 cm, thickness 3 mm) supplied by Goodfellow (U.K.) and Weber Métaux (France), respectively. Before treatment, they were polished first on abrasive paper (P4000, Presi, France) and then on a wet cloth (DP-Nap, Struers, France) until a shiny "mirror" surface was obtained. They were rinsed in water and then acetone under sonication for 5 min and dried in an oven (80 °C, overnight).

For the PTFE reduction in a DMF solution, tetrabutylammonium tetrafluoroborate was used as the electrolyte; it was synthesized from ammonium tetrafluoroborate and tetrabutylammonium chloride (Fluka, France) and recrystallized in petroleum ether.[32] DMF (puriss, Fluka) was used as received.

The other chemical reagents were purchased from Aldrich (Saint-Quentin Fallavier, France) and used as received.

Platinum wires, used in the ultramicroelectrodes, were of 99.9% purity (Goodfellow, U.K.). Ultramicroelectrode (UME) tips were obtained according to the literature.[29]

The platinum microelectrode tip [metallic radius $a = 12.5$ $\mu$m; $6 < RG < 10$ (RG = ratio of glass to metallic radii)], a platinum counterelectrode (radius 0.5 mm), and an anodized Ag/AgCl reference wire (radius 0.5 mm) without any reference compartment were placed in 5 mL of DMF. We have checked that, for the different tips we have used, the experimental approach curve of an insulating substrate followed the theoretical one predicted for RG = 10. The fluoropolymer sample was held on the bottom of a glass cell. The microelectrode tip was moved by a horizontal or a vertical translation stage (speed 0.5, 1, or 2 $\mu$m/s) driven by an electrical microstep motor piloted by a computer (CMA motors driven by an ESP300, Newport).

The solution typically contained the supporting electrolyte, $NBu_4BF_4$, and two redox mediators, $P_1$ and P, where $[P_1] < 0.1[P]$. $P_1$ was chosen so that it did not induce the polymer carbonization ($P_1$ is phthalonitrile for PTFE and nitrobenzene for PCTFE, Table 1). The standard reduction potentials of the redox mediators given in Table 1 have been measured relative to those of our reference electrode and nitrobenzene, whose $E°$ is −1.08 V vs SCE.[33]

The positioning of the microelectrode was done by recording the microelectrode reduction current of $P_1$, $i_T$, as a function of the fluoropolymer plaque−microelectrode distance, $d$.[34] During this first approach curve, the microelectrode potential was set on the reduction plateau of $P_1$ and its current followed the approach curve of an insulating substrate. The tip was then positioned so that $i_T/i_{T,\infty} \approx 0.4$ (with $i_{T,\infty} = 4nF[P_1]Da$, the current at infinite distance with $[P_1]$ the bulk concentration of $P_1$), which corresponded to $d \approx 7.5$ $\mu$m.[29,30]

The tip was pulled back a known distance from the substrate. The microelectrode potential was then set on the reduction plateau of P, and the current−time curve was converted into the approach curve of the substrate with the redox mediator P. This technique led to a precision in the tip−surface distance better than 0.5 $\mu$m.

Potentials were imposed and currents measured by a potentiostat/galvanostat (CH660A, CH Instruments, U.S.).

The solution was degassed with nitrogen for 10 min before use, and the whole device was kept under nitrogen in a polyethylene bag (glovebag, Aldrich) during the experiment. The humidity in the plastic bag was maintained as low as possible, RH < 0.3, with molecular sieves; this was checked by a hair hygrometer.

## 3. Results and Discussion

Approach curves represent the evolution of the dimensionless tip current $I_T = i_T/i_{T,\infty}$ as a function of the normalized electrode−substrate distance $d/a$, where $i_T$ is the tip current, $i_{T,\infty}$ its value measured at infinite distance from the substrate, $d$ the electrode−substrate distance, and $a$ the microelectrode tip radius. We have obtained approach curves toward the PTFE or the PCTFE surface under different experimental conditions by changing the concentration and the nature of the redox mediator. Two types of substrates were studied with this method: the virgin fluoropolymer and the carbonaceous domain obtained by the reduction of the latter using the SECM (modified fluoropolymer).

**3.1. Approach Curves on PTFE and PCTFE.** Figure 2 shows the curves obtained for different radical anions, $P^{\bullet -}$, electrogenerated at a microtip (radius $a = 12.5$ $\mu$m) approaching the virgin PTFE substrate. The microtip was biased to a potential sufficiently negative to reduce the mediator P to $P^{\bullet -}$ within mass-transfer control. Different situations were observed according to the standard reduction potential of the mediator, $E_P°$. They resulted in varying amounts of carbonized PTFE.

First, the three most negative mediators ($E_P° < -2.1$ V vs ECS) exhibit similar approach curves over the PTFE substrate although they span over a ca. 200 mV potential region. This indicates that the regeneration of these mediators at the PTFE-carbonized surface was controlled by finite potential-independent heterogeneous kinetics. The situation is different for redox mediators with a reducing power lower than that of the 2,2′-dipyridyl radical anion (−2.1 V vs SCE $< E_P° <$ −1.6 V vs SCE). In this case, regeneration was much lower and presented a dependency on the potential. No regeneration was observed when $E_P°$ was higher than −1.6 V vs SCE, the experimental approach curve resembled that of an insulating substrate with a tip having a RG = 10, and no carbonization of the PTFE was observed in this region.

In the range of mediators used, reduction induced carbonization of the polymer and it was impossible to fit the experimental approach curves with the theoretical equations established for

**TABLE 1: Redox Mediators**

| redox mediator, P | $E_P^\circ$ [a] (V vs SCE) | redox mediator, P | $E_P^\circ$ [a] (V vs SCE) | redox mediator, P | $E_P^\circ$ [a] (V vs SCE) |
|---|---|---|---|---|---|
| nitrobenzene | −1.08 | anthracene | −1.90 | 2,2′-dipyridyl | −2.10 |
| phthalonitrile | −1.59 | 2,4′-bipyridine | −1.95 | benzonitrile | −2.26 |
| 4,4′-dipyridyl | −1.81 | phenanthridine | −2.03 | naphthalene | −2.43 |

[a] $E^\circ$ of the redox reaction $P + e^- \rightarrow P^{\bullet -}$; see the Experimental Section for its estimation.

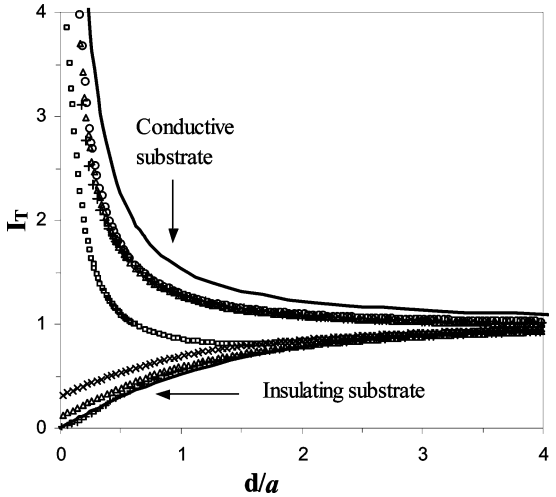


**Figure 2.** Approach curves for the reduction of a 50 mM concentration of a redox mediator, P, in DMF + 0.1 M $NBu_4BF_4$ at a Pt UME (radius $a$ = 12.5 $\mu$m) approaching a PTFE surface (1 $\mu$m/s). From top to bottom: experimental approach with P = benzonitrile (○), 2,2′-dipyridyl (△), phthalonitrile approaching the reduced PTFE surface (+), phenanthridine (□), 2,4′-dipyridyl (×), 4,4′-dipyridyl (△), and phthalonitrile (+). The solid lines correspond to the theoretical approach of a conductive (top) and an insulating (bottom) surface.

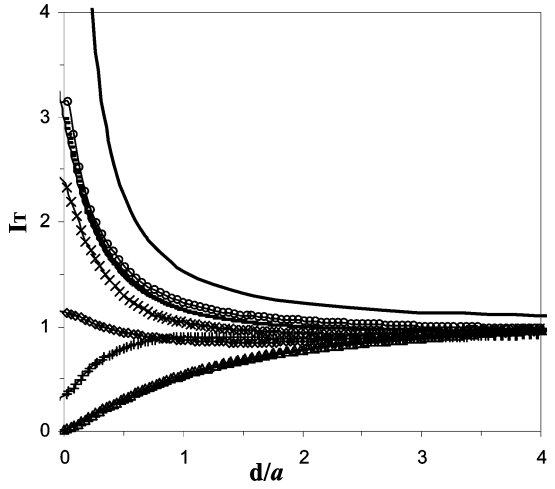


**Figure 3.** Approach curves for the reduction of a 50 mM concentration of a redox mediator, P, in DMF + 0.1 M $NBu_4BF_4$ at a Pt UME ($a$ = 12.5 $\mu$m) approaching a PCTFE surface (1 $\mu$m/s). From top to bottom: experimental approach with P = benzonitrile (○), 2,2′-dipyridyl (−), 2,4′-dipyridyl (×), 4,4′-dipyridyl (◇), phthalonitrile (+), and nitrobenzene (△). The solid lines correspond to the theoretical approach curves of a conductive (top) and an insulating (bottom) surface.

the characterization of a finite heterogeneous electron transfer.[35,36] This could be interpreted as the consequence of a time-dependent phenomenon interacting with the heterogeneous electron transfer. The occurrence of time-dependent phenomena while the approach curves were obtained was confirmed by some simple observations given below.

For the most positive reducing agents, the building of the carbonized area required reduction times as long as several minutes.

Conversely, for the three most reducing mediators, we have observed that the carbonized area regenerated at a sufficient and almost constant rate after ∼20 s at a normalized distance $d/a = 0.56$. In this case, the carbonized area was built during the beginning of the approach (at 0.5, 1, or 2 $\mu$m/s), giving rise to an increasing feedback for longer times as the microelectrode approached the surface. As soon as the tip was within 10−20 $\mu$m ($d/a \approx 1 - 1.5a$) from the substrate, the carbonized area had already been built and the mediator regeneration became potential and time independent. Therefore, at long distances ($d/a > 4-6$ depending on the scan rate), the approach curves resembled those obtained for an insulating substrate, and at short distances ($d/a < 1 - 1.5a$), they tended toward a limit that was the same for the three mediators, as observed in Figure 2. In the intermediate zone during which the carbonized area is built ($3 < d/a < 5$), the approach curve presented a light hollow (where the current passes through a minimum, not shown, out of the range of Figure 2) as has previously been observed when time-dependent phenomena are interacting with the heterogeneous regeneration of the redox mediator.[37] The hollow reflects the transition between a mass-transfer control by the hindrance of the redox mediator diffusion toward the tip (negative feedback of the insulating behavior) and the regeneration of the mediator by the substrate. For higher speeds of the microelectrode, this hollow was observed closer to the polymer surface as expected: at $d/a$ = 3.3, 4.1, and 4.7 when the speed was 2, 1, and 0.5 $\mu$m/s, respectively. We believe that the interacting limiting phenomenon affecting the kinetics corresponds to the nucleation and growth of the carbonized area.

A better understanding and analysis of the time-dependent growth phenomenon would imply a study under static conditions in a collection-generation mode. This is the aim of a forthcoming paper.

Figure 3 represents the approach curves obtained for different radical anions electrogenerated at a microtip approaching the virgin PCTFE substrate. Similar observations were made concerning the potential dependency of the approach curves. In this case, only the radical anion of nitrobenzene did not induce the PCTFE carbonization. Again none of the experimental curves could be fit by the finite heterogeneous kinetics model, except that of nitrobenzene, which fit the approach of an insulating substrate.

The fact that PCTFE reduction was initiated at a more positive potential than that of PTFE is related to the easier reduction of chloroalkanes compared to fluoroalkanes. The same trend is generally observed during the reduction of molecular compounds within the haloalkane series as a consequence of the difference in the C−X bond strengths.[38,39]

**3.2. Potential Dependency of the Fluoropolymer Reduction.** Since no fitting procedure could be used, we have attempted a more detailed analysis of the polymer reduction process from the approach curves by comparing the currents, for a given distance between the tip and the substrate, for different $E_P^\circ$ values. Indeed, for electrochemical processes

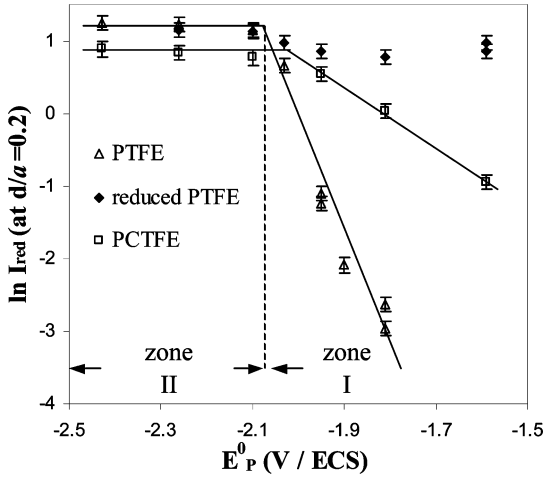


**Figure 4.** Variation of the substrate reduction current, $I_{red}$, obtained from $I_T$ (eq 5) at a tip−subtrate distance of $0.2a$, with the standard reduction potential of the redox mediator P, $E_P°$ (Pt UME, $a = 12.5$ $\mu$m). The substrates (△) PTFE, (□) PCTFE, and (◆) carbonaceous material resulting from PTFE reduction were reduced by the radical anion of P = (from left to right) naphthalene, benzonitrile, 2,2′-dipyridyl, phenanthridine, 2,4′-dipyridyl, 4,4′-dipyridyl, and phthalonitrile.

limited by a heterogeneous electron transfer at the liquid−solid interface, in a thin-layer configuration, an estimate of $\pi k_{het} a/4D$ may be given by the value of the current at small electrode separations ($d \ll a$).[40] We believe that, under our experimental conditions, $d = 0.2a$ is the smallest distance that we were able to reproduce reasonably without any physical contact.

The current used to reduce PTFE, $i_{red}$, was deduced from the tip current, $i_T$, taken at the normalized distance $L = d/a = 0.2$. For that, the simple formalism developed by Mirkin was used:[35] knowing the tip currents under the negative and positive pure feedbacks (obtained from the approach of, respectively, an insulating or a conductive substrate), namely, $i_{T,ins}$ and $i_{T,c}$, an estimate of the normalized current flowing through the substrate, $I_S = I_{red}$, is given by

$$I_T = I_S(1 - I_{T,ins}/I_{T,c}) + I_{T,ins} \quad (5)$$

where the different $I$ values refer to the currents normalized according to the value at the tip held at a large distance from the substrate, which may be viewed as infinite since the tip does not probe the substrate: $I = i/i_{T,\infty}$, with $i_{T,\infty} = 4nF[P]Da$, and $I_{T,ins}$ and $I_{T,c}$ are given by[29]

$$I_{T,ins} = 1/(0.15 + 1.5358/L + 0.58\exp(-1.14/L) + 0.0908\exp[(L - 6.3)/(1.017L)]) \quad (6)$$

$$I_{T,c} = 0.78377/L + 0.3315\exp(-1.0672/L) + 0.68 \quad (7)$$

with $L = d/a$.

Figure 4 presents the variation of $I_{red}$ with the mediator standard reduction potential, $E_P°$ in the case of PTFE and PCTFE reduction. Two different kinetic regimes were clearly evidenced according to $E_P°$ values. For mediators having $E_P° > E_{lim}°$, where $E_{lim}° = -2.1$ V vs SCE for PTFE and $-2.03$ for PCTFE, the logarithm of the current increased linearly when the mediator reduction potential decreased. This potential region is denoted the low driving force region since the more positive $E_P°$, the less favored the polymer reduction and then the lower the driving force available for this reduction. Conversely, for mediators with more negative potentials, more driving force is available for the polymer reduction that is independent of the mediator potential. This potential region is denoted the high driving force region.

*3.2.1. Zone I: $E_P° > E_{lim}°$.* The potential dependency of the polymer reduction gives interesting information on the reduction mechanism. Since, in a first approximation, the reduction current is proportional to $k_{het}$, the charge transfer at the solution−polymer interface rate constant, the potential dependency of the current reflects the potential dependency of $k_{het}$.

The reduction scheme is difficult to envision precisely. However, two situations may be distinguished.

In the first situation, the radical anion, $P^{\bullet -}$, transfers its electron, according to reaction 8, to the already carbonized polymer $-(C-)_n$, denoted as the phase $\varphi 1$. The conductivity

$$-(C-)_n + (n\delta)P^{\bullet -} + (n\delta)NBu_4^+ \rightarrow -(C^{\delta -}-,\delta NBu_4^+)_n + (n\delta)P \quad (8)$$

of the carbonized polymer (discussed in section 3.3) may be sufficient for it to behave as an electrode material and transport the charge ($e^-_{\varphi 1}$) toward the carbonized polymer−fluoropolymer interface, where the electron is transferred to the fluoropolymer (denoted phase $\varphi 2$) to induce its reduction, according to

$$-(CF_2-CFX)_{n-\varphi 2} + e^-_{\varphi 1} \rightarrow \text{products}$$

In this case, $k_{het}$ would describe the ET for the fluoropolymer macromolecule reduction at an electrode-like phase (the phase $\varphi 1$) whose potential is fixed by the $E_P°$ of the redox mediator.

In the second situation, the carbonaceous material has a porous structure in which the radical anion may diffuse toward the PTFE interface, where the ET occurs

$$-(CF_2-CFX)_{n-\varphi 2} + P^{\bullet -}_{\varphi 1} \rightarrow P_{\varphi 1} + \text{products}$$

where the phase $\varphi 1$ is more likely a liquid phase that fills the carbonaceous material pores. In this latter situation, the $k_{het}$ value would depict the ET for the fluoropolymer reduction at a "liquid"−"polymer" interface and might parallel the ET at liquid−liquid interfaces.

Finally the real situation may be a mix of those two limiting cases. However, in any of those situations, the potential dependency of the polymer reduction current may describe the dynamics of the interfacial ET transfer to the fluorpolymer macromolecule and could be described by an apparent electron-transfer coefficient, $\alpha$.

The reduction of a monomeric unit of PTFE or PCTFE involves four electron transfers from $P^{\bullet -}$ and the breaking of four C−X bonds in agreement with eq 1:

$$-(CF_2-CFX)- + 4P^{\bullet -} \rightarrow -(CC)- + 3F^- + X^- + 4P \quad (9)$$

X = F for PTFE and X = Cl for PCTFE.

This global reduction by a total exchange of four electrons has been decomposed into three contributions, $n$, $r$, and $s$, corresponding to the kinetic limiting step ($n$), the step before ($r$), and the step after ($s$), with $n + r + s = 4$.

The data were then analyzed as a Tafel plot, and from the slope, the apparent transfer coefficient of the interfacial ET to the fluoropolymer, $\alpha$, of the rate-limiting step could be defined as[41]

$$\alpha n + r = \partial\Delta G^{\ddagger}/\partial\Delta G° \quad (10)$$

where $\Delta G^{\ddagger}$ is the free energy barrier of this ET and $\Delta G^{\circ}$ its driving force.

The free energy barrier under SECM conditions is roughly the reduction current passing through the solution−PTFE interface. The driving force should include the difference, $E_P^{\circ} - E_{pol}^{\circ}$, between the standard reduction potentials of the mediator and the polymer, but also an interfacial potential drop, denoted as $\Delta\phi$, corresponding to ion transfer from the phase $\varphi 1$ to the polymeric one, $\varphi 2$:

$$\Delta G^{\circ} = -F(E_P^{\circ} - E_{pol}^{\circ} - \Delta\phi)$$

Since the experiments were performed under a constant electrolytic concentration, the slope of the plot in Figure 4 should give an estimate of the electron-transfer coefficient as

$$\alpha n + r = (RT/F)\, \mathrm{d}(\ln I_{red})/\mathrm{d}E_P^{\circ} \qquad (11)$$

This value characterizes the potential dependency of electron transfer to the polymer; it is 0.42 for PTFE and 0.11 for PCTFE. A refinement of these values would consist in estimating the minimal values $k_{het}$ that would lead to similar values according to the finite kinetic approach.[35] The minimal value of $k_{het}$ is deduced from the value of $I_{red}$ at $L = 0.2$, from the resolution of

$$I_{red} = I_S = 0.78377/(L(1 + 1/\Lambda)) + [0.68 + 0.3315 \exp(-1.0672/L)]/[1 + F(L,\Lambda)] \qquad (12)$$

with

$$F(L,\Lambda) = (11 + 7.3\Lambda)/(\Lambda(110 - 40L)) \qquad (13)$$

and $\Lambda = k_{het}d/D$.

The ensuing values of $\alpha n + r$ are 0.49 and 0.15 for PTFE and PCTFE, respectively. They indicate that the first electron-transfer step for both polymers' reduction is rate determining ($r = 0$).

We have compared those results to those for electron transfers to halogenated molecules. In the aliphatic series, it has been demonstrated that the rate-limiting step was the first exchange of one electron.[39]

For general aliphatic chloroalkanes,[39] or even chlorofluorocarbons such as $CF_3Cl$,[42] the first electron transfer is concerted with the breaking of the C−Cl bond; the electron transfer is called dissociative:

$$RCl + e \rightarrow R^{\bullet} + Cl^{-} \qquad (14)$$

Conversely, in the case of a perfluorinated model compound $R_fF$ such as perfluorodecalin, the first electron transfer is nondissociative and leads to a radical anion:[43]

$$R_fF + e \rightarrow R_fF^{\bullet -} \qquad (15a)$$

Then, the C−F bond breaking occurs at the level of the radical anion:

$$R_fF^{\bullet -} \rightarrow R_f^{\bullet} + F^{-} \qquad (15b)$$

If the same $n = 1$ holds for PTFE and PCTFE reductions, the rate-limiting step is also the first electron transfer to a monomeric unit of the perfluoralkyl chain according to

$$-(CF_2-CFX)_m-CF_2-CFX-(CF_2-CFX)_q + e \rightarrow -(CF_2-CFX)_m-CF_2-CFX^{\bullet -}(CF_2-CFX)_q \qquad (16)$$

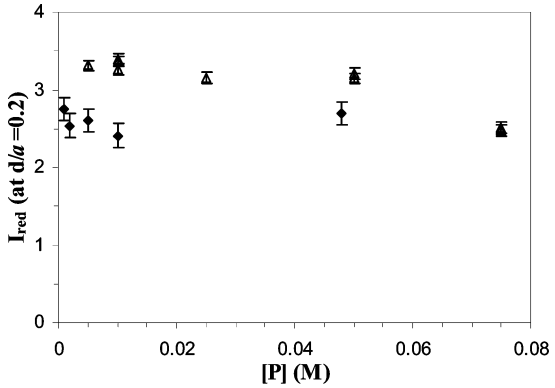


**Figure 5.** Variation of $I_T$, the current for reduction of P, with mediator concentration at an UME tip held at $d = 0.2a$ of a PTFE or a reduced PTFE surface (Pt UME, $a = 12.5\ \mu$m). P = (△) 2,2′-dipyridyl, approach to PTFE, and (◆) phthalonitrile, approach to reduced PTFE.

or

$$-(CF_2-CFX)_m-CF_2-CFX-(CF_2-CFX)_q + e \rightarrow -(CF_2-CFX)_x-CF_2-CF^{\bullet}-(CF_2-CFX)_q + X^{-} \qquad (17)$$

depending on whether the electron transfer is concerted with the breaking of the C−X (X = F or Cl) bond.

The value of $\alpha \approx 0.45$ would indicate that PTFE is reduced according to eq 16 in a nondissociative fashion, in agreement with the behavior of perfluorodecalin. On the contrary, the value of the apparent electron-transfer coefficient for PCTFE reduction would rather be in favor of the dissociative mechanism (eq 17) as reported in solution for chloroalkanes.[39,44]

*3.2.2. Zone II: $E_P^{\circ} < E_{lim}^{\circ}$.* For mediators with lower reduction potentials, a second kinetic regime was obtained where the reduction process was almost potential independent. We have also observed that, in this potential area, the approach curve of PTFE was independent of the supporting electrolyte and the redox mediator concentrations in the range $0.015\ \mathrm{M} \le [NBu_4^+] \le 0.2\ \mathrm{M}$, with $[NBu_4^+] \ge 0.6[P]$ and $[P] \le 0.05$ M (Figure 5, △). For the highest values of [P], the feedback of the surface was less important since the substrate may not support high currents provided by such high concentrations. It corroborates the high current regime observed in the microband electrode configuration.[26] In such potential regions, the approach curves do not reflect the growth limitation of the carbonaceous layer by the PTFE reduction (eq 9) kinetics anymore. It corresponds to the limitation by the charging kinetics and conductivity of the carbonaceous material, symbolized by eq 8.

**3.3. Reduction of Carbonized PTFE.** We have investigated the extent of reduction for the carbonaceous material formed by the PTFE reduction. For that purpose, approach curves were drawn on a PTFE area freshly reduced by the redox mediator of 2,2′-dipyridyl.

Indeed, it is interesting to note in Figure 2 that the approach curves performed on PTFE with highly reducing radical anions were similar to the approach curves toward the reduced PTFE when using the radical anion of the least reducing mediator (phthalonitrile, symbol +). A similar behavior was also observed when a carbonized zone with radical anions that did not give rise to a high feedback was approached. The likeliness of the curves confirms that, at a high driving force, the fluoropolymer reduction is controlled by the dynamics of the reduction of the carbonaceous layer (eq 8).

Different approach curves of the carbonized PTFE area are shown in Figure 6, with the theoretical (obtained from combination of eqs 5−7, 13, and 14) approach of a substrate that enabled

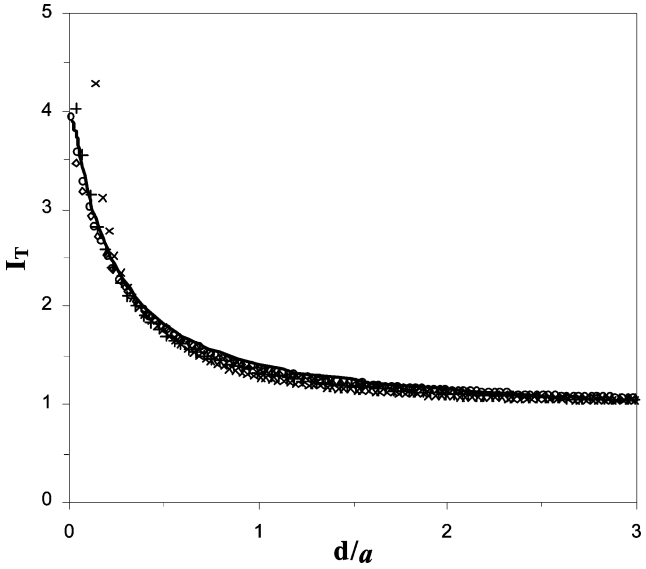


**Figure 6.** Approach curves for the reduction of 20 mM phthalonitrile in DMF at a Pt UME ($a = 12.5$ $\mu$m) approaching a reduced PTFE surface (PTFE reduction was achieved by an SECM in a solution of 50 mM 2,2′-dipyridyl during 400 s). The solid line corresponds to the best fitting according to ref 35 with $k_{het} = 0.04$ cm s$^{-1}$. The different symbols refer to different approaches.

regeneration with a finite heterogeneous kinetic rate constant, $k_{het} = 0.04$ cm s$^{-1}$. These show that the curves are dependent, to some extent, on the nature of the material formed by the PTFE reduction. Moreover, the simple kinetic model of finite heterogeneous kinetics roughly fits the experiments. Similar incompatibilities have also been observed when conducting polypyrrole films electrodeposited on electrodes have been characterized by the SECM.[40b]

The values of the reduction current, $I_{red}$, obtained at $d/a = 0.2$ are reported in Figure 4 as a function of the mediator standard potential (◆) or in Figure 5 as a function of the redox mediator concentration (◆). We notice that the SECM characterization for the electrochemical properties of the carbonaceous layer was almost independent of the potential and the supporting electrolyte or the redox mediator concentrations for 0.015 M < [$NBu_4^+$] < 0.2 M, [$NBu_4^+$] > 2[phthalonitrile], and [phthalonitrile] < 0.05 M. We have not tested other concentration ranges, but those arguments would be in favor of a kinetic limitation by charge transport into the reduced PTFE layer as postulated in earlier works.[1,26]

Actually the approach curve was particularly dependent on the extent of water contamination of the solution. We believe the carbonaceous layer to be particularly sensitive to a great number of electrophiles. The approach curve would then reflect the chemical stability of the carbonaceous layer. We have not attempted to investigate such effect in detail; however, the conductive behavior of the reduced PTFE leads to $k_{het}$ values equal to or greater than 0.04−0.1 cm s$^{-1}$. The SECM characterization of the conductivity of the reduced fluoropolymer is comparable to what has been observed for conductive polymers.[40b,45]

Similar behavior was observed on the carbonaceous areas formed by PCTFE reduction. However, as already observed in the high driving force region of the polymer reduction, the reduced PCTFE was less conductive than the reduced PTFE. This may be related to structural differences in the materials. Indeed, the concentration of monomeric units was higher for PTFE (22.2 M) over PCTFE (17.6 M). Lower concentration should facilitate ion transport into the reduced matrix but could also result in more chain scissions and henceforth in the lower conductivity of the reduced material. Such rearrangements may also explain why both reduced fluoropolymers did not show pure positive feedback.

## Conclusion

We have demonstrated that fluoropolymers were easily reduced by an SECM in the feedback mode. The approach curves indicated the presence of a time-dependent phenomenon attributed to the growth of the chemical transformation (reduction) of the polymer into a conductive, carbonaceous material. From the variation of tip current at a small tip−substrate separation with the redox mediator standard potential, we have demonstrated the existence of two kinetic regimes. The global material reduction may be controlled either by, at low driving force (most positive redox mediator standard potentials), the potential-dependent reduction of the fluoropolymer into carbon (symbolized by the global eq 9) or, at higher driving force, by the intrinsic conductivity of the carbonaceous material in which charges propagate (eq 8). The potential dependency of the current reduction obtained at low driving force demonstrates that the fluoropolymer reduction depends on its chemical nature. The chlorinated polymer surface was easier to reduce than the fluorinated one, in agreement with the trends observed in organic solution electrochemistry. Moreover, a value of the apparent transfer coefficient close to 0.5 was obtained for $CF_2CF_2$ units, and a much lower value of 0.11 was observed for $CF_2CFCl$. Such differences are parallel to those observed in organic electrochemistry in solution, and the dissociative nature of the first electron transfer could be invoked.

The conductivity of the carbonaceous material has been investigated by the SECM. It depends also on the nature of the fluoropolymer that had been used for its formation. It is moderately conductive ($k_{het} \approx 0.05$ cm s$^{-1}$) but greatly sensitive to the extent of water and oxygen in the solution. Nonetheless, its conductivity is high enough to involve the *n*-doped carbonaceous material in successive redox reactions and induce the local metalization[46] and grafting[47] of the polymer.

In a forthcoming paper we will discuss transient results obtained in the SECM configuration, to depict the reductive growth of the carbonized zone with time.

## References and Notes

(1) Kavan, L. In *Chemistry and Physics of carbon*; Thrower, P. A., Ed.; Marcel Dekker: New York, 1991; Vol. 23, pp 71−171. (b) Kavan, L. *Chem. Rev.* **1997**, *97*, 3061.
(2) Brewis, D. M.; Dahm, R. H. *Int. J. Adhes. Adhes.* **2001**, *21*, 397.
(3) Jansta, J.; Dousek, F. P. *Electrochim. Acta* **1973**, *18*, 673.
(4) Brecht, H.; Mayer, F.; Binder, H. *Angew. Makromol. Chem.* **1973**, *33*, 89.
(5) Dwight, D. W.; Riggs, W. M. *J. Colloid Interface Sci.* **1974**, *47*, 650.
(6) Riggs, W. M.; Dwight, D. W. *J. Electron Spectrosc. Relat. Phenom.* **1974**, *5*, 447.
(7) Dousek, F. P.; Jansta, J. *Electrochim. Acta* **1975**, *20*, 1.
(8) Jansta, J.; Dousek, F. P.; Riha, J. *J. Appl. Polym. Sci.* **1975**, *19*, 3201.
(9) Dahm, R. H.; Barker, D. J.; Brewis, D. M.; Hoy, L. R. J. *Adhesion*; Applied Science: London, 1980; Vol. 4, p 215.
(10) Barker, D. J.; Brewis, D. M.; Dahm, R. H.; Gribbin, J. D.; Hoy, L. R. J. *J. Adhes.* **1981**, *13*, 67.
(11) Dahm, R. H. *Surface Analysis and Pretreatmnt of Plastics and Metals*; Applied Science: London, 1982; p 227.
(12) Fouletier, M. Ph.D. Thesis, Grenoble, 1983.
(13) Fouletier, M.; Armand, M. Fr. Pat. 2552092, 1983; *Chem. Abstr.* **1985**, *103*, P178814b.
(14) Kavan, L.; Bastl, Z.; Dousek, F. P.; Jansta, J. *Carbon* **1984**, *22*, 77.
(15) Ge, P. Synthesis and functionalization of carbon Ex-PTFE. Ph.D. Thesis, Grenoble, 1987.

(16) Combellas, C.; Kanoufi, F.; Thiébault, A.; Delamar, M.; Bertrand, P. *Polymer* **1999**, *40*, 2011.
(17) Nelson, E. R.; Kilduff, T. J.; Benderly, A. A. *Ind. Eng. Chem.* **1985**, *50*, 329.
(18) Jansta, J.; Dousek, F. P.; Patzelova, V. *Carbon* **1975**, *13*, 377.
(19) Barker, D. J.; Brewis, D. M.; Dahm, R. H.; Hoy, L. R. J. *Polymer* **1978**, *19*, 856.
(20) Jansta, J.; Dousek, F. P. *Electrochim. Acta* **1981**, *26*, 233.
(21) Yoshino, K.; Yanagida, S.; Sakai, T.; Azuma, T.; Inuishi, Y., Sakurai, H. *Jpn. J. Appl. Phys.* **1982**, *21*, L301.
(22) Kavan, L.; Dousek, F. P.; Weber, J.; Micka, K. *Carbon* **1988**, *26*, 235.
(23) Kavan, L.; Dousek, F. P.; Weber, J.; Micka, K. *Carbon* **1988**, *26*, 245.
(24) Kavan, L.; Dousek, F. P.; Micka, K. *J. Phys. Chem.* **1990**, *94*, 5127.
(25) Kavan, L.; Dousek, F. P.; Micka, K. *Solid State Ionics* **1990**, *38*, 109.
(26) Amatore, C.; Combellas, C.; Kanoufi, F.; Sella, C.; Thiébault, A.; Thouin, L. *Chem.—Eur. J.* **2000**, *6*, 820.
(27) Bard, A. J.; Fan, F.-R. F.; Kwak, J.; Lev, O. *Anal. Chem*. **1989**, *61*, 132.
(28) Bard, A. J.; Denuault, G.; Lee, C.; Mandler, D.; Wipf, D. O. *Acc. Chem. Res*. **1990**, *23*, 357.
(29) Bard, A. J.; Fan, F.-R. F.; Mirkin, M. V. In *Electroanalytical Chemistry*; Bard, A. J., Ed.; Marcel Dekker: New York, 1994; Vol. 18, p 243.
(30) *Scanning Electrochemical Microscopy*; Bard, A. J., Mirkin, M. V., Eds.; Marcel Dekker: New York, 2001.
(31) Treichel, D.; Mirkin, M. V.; Bard, A. J. *J. Phys. Chem.* **1994**, *98*, 5751.
(32) Amatore, C.; Azzabi, M.; Calas, P.; Jutand, A.; Lefrou, C.; Rollin, Y. *J. Electroanal. Chem*. **1990**, *288*, 45.
(33) Andrieux, C. P.; Gelis, L.; Médebielle, M.; Pinson, J.; Savéant, J.-M. *J. Am. Chem. Soc.* **1990**, *112*, 3509.
(34) Kanoufi, F.; Combellas, C.; Shanahan, M. E. R. *Langmuir* **2003**, *19*, 6711.
(35) Wei, C.; Bard, A. J.; Mirkin, M. V. *J. Phys. Chem.* **1995**, *95*, 16033.
(36) Mirkin, M. V. In *Scanning Electrochemical Microscopy*; Bard, A. J., Mirkin, M. V., Eds.; Marcel Dekker: New York, 2001; Chapter 5, p 145.
(37) (a) Unwin, P. R.; Bard, A. J. *J. Phys. Chem.* **1991**, *95*, 7814. (b) Barker, A. L.; Unwin, P. R.; Amemiya, S.; Zhou, J.; Bard A. J. *J. Phys. Chem. B* **1999**, *103*, 7260. (c) Kanoufi, F.; Cannes, C.; Zu, Y.; Bard, A. J. *J. Phys. Chem. B* **2001**, *105*, 8951.
(38) Peters, D. G. In *Organic Electrochemistry*, 3rd ed.; Lund, H., Baizer, M. M., Eds.; Marcel Dekker: New York, 1991; p 361.
(39) (a) Savéant, J.-M. *J. Phys. Chem*. **1994**, *98*, 3716. (b) Savéant, J.-M. In *Advances in Electron-Transfer Chemistry*; JAI Press Inc.; 1994; Vol. 4, pp 53−116. (c) Savéant, J.-M. *Tetrahedron* **1994**, *50*, 10117. (d) Savéant, J.-M In *Advances in Physical Organic Chemistry*; Tidwell, T. T., Ed.; Academic Press: New York, 2000; Vol. 35, pp 117−192.
(40) (a) Mirkin, M. R.; Arca, M.; Bard, A. J. *J. Phys. Chem.* **1993**, *97*, 10790. (b) Arca, M.; Mirkin, M. R.; Bard, A. J. *J. Phys. Chem.* **1995**, *99*, 5040.
(41) *Modern Electrochemistry*; Bockris, J. O.; Reddy, A. K. N., Eds.; Plenum: New York, 1970; Vol. 2, Chapter 9.
(42) Bertran, J.; Gallardo, I.; Moreno, M.; Savéant, J.-M. *J. Am. Chem. Soc.* **1992**, *114*, 9576.
(43) Combellas, C.; Kanoufi, F.; Thiébault, A. *J. Phys. Chem. B* **2003**, *107*, 10894.
(44) Maran, F.; Wayner, D. D. M.; Workentin, M. S. In *Advances in Physical Organic Chemistry*; Tidwell, T. T., Ed.; Academic Press: New York, 2000; Vol. 36, pp 85−166.
(45) (a) Tsionsky, M.; Bard, A. J.; Dini, D.; Decker, F. *Chem. Mater*. **1998**, *10*, 2120. (b) Quinto, M.; Bard, A. J. *J. Electroanal. Chem.* **2001**, *498*, 67.
(46) Combellas, C.; Kanoufi, F.; Mazouzi, D.; Thiébault, A. *J. Electroanal. Chem.* **2003**, *556*, 43.
(47) Combellas, C.; Kanoufi, F.; Mazouzi, D.; Thiébault, A.; Bertrand, P.; Médard, N. *Polymer* **2003**, *44*, 19.